AIP | The Journal of Chemical Physics

Structure and properties of Mn4Cl9: An antiferromagnetic binary hyperhalogen

Yawei Li, Shunhong Zhang, Qian Wang, and Puru Jena

Citation: J. Chem. Phys. **138**, 054309 (2013); doi: 10.1063/1.4776217
View online: http://dx.doi.org/10.1063/1.4776217
View Table of Contents: http://jcp.aip.org/resource/1/JCPSA6/v138/i5
Published by the American Institute of Physics.

Structure and properties of Mn_4Cl_9: An antiferromagnetic binary hyperhalogen

Yawei Li,[1] Shunhong Zhang,[1] Qian Wang,[1,2,a)] and Puru Jena[2]
[1]*Center for Applied Physics and Technology, College of Engineering, Peking University, Beijing 100871, China*
[2]*Department of Physics, Virginia Commonwealth University, Richmond, Virginia 23284, USA*

(Received 26 October 2012; accepted 2 January 2013; published online 7 February 2013)

Calculations based on density functional theory show that the structure of Mn_4Cl_9 anion is that of a Mn atom at the core surrounded by three $MnCl_3$ moieties. Since Mn is predominantly divalent and $MnCl_3$ is known to be a superhalogen with a vertical detachment energy (VDE) of 5.27 eV, Mn_4Cl_9 can be viewed as a hyperhalogen with the formula unit $Mn(MnCl_3)_3$. Indeed, the calculated VDE of Mn_4Cl_9 anion, namely 6.76 eV, is larger than that of $MnCl_3$ anion. More importantly, unlike previously discovered hyperhalogens, Mn_4Cl_9 is the first such hyperhalogen species composed of only two constituent atoms. We further show that Mn_4Cl_9 can be used as a ligand to design molecules with even higher VDEs. For example, $Li[Mn(MnCl_3)_3]_2$ anion has a VDE of 7.26 eV. These negatively charged clusters are antiferromagnetic with most of the magnetic moments localized at the Mn sites. Our studies show new pathways for creating binary hyperhalogens. © *2013 American Institute of Physics*. [http://dx.doi.org/10.1063/1.4776217]

INTRODUCTION

Atoms, molecules, and clusters with high electron affinities (EA) are promising candidates for oxidizing systems with relatively high ionization potentials, and for the synthesis of organic superconductors as well as high energy density salts with unusual stability and desired properties.[1–3] For example, the first compound containing noble gas atom, $Xe^+[PtF_6]^-$,[4] was synthesized by Bartlett using PtF_6, the EA of which was estimated to be about 7.00 eV,[5] much larger than that of the Cl atom (3.617 ± 0.003 eV).[6] In 1981, Gutsev and Boldyrev coined the term superhalogen to describe such molecules and showed[7] that these molecules could be created with the formula MX_{k+1} where M is a metal atom with maximal valence k and X is a halogen atom.[7] The vertical detachment energies (VDEs) of MX_{k+1}^- were found to greatly exceed those of the halogen anions due to the delocalization of the additional electron over all the X atoms instead of a single X atom.[8] Since then, numerous theoretical[9–22] as well as experimental[23–30] efforts have been devoted to find superhalogen anions with high VDE values. Much of the early work, however, concentrated on having a single metal atom at the core surrounded by halogen atoms. It was later shown that superhalogens can also be formed where the core consisting of a single metal atom is replaced by a metal-halogen complex. Since MX_k has a closed shell, it is natural to expect that the clusters with the formula of $(MX_k)_n$ will exhibit singlet ground-states. Based on calculations and photoelectron spectroscopy (PES),[31] Boldyrev and Wang found M_nX_{nk+1} clusters form superhalogens, where M can be an alkaline and alkaline earth atom.[32,33] In such polynuclear superhalogens, the EA increases with the size of the core. These findings paved the way to design new systems, namely, $H_{12}F_{13}^-$ with a very large VDE value of 13.87 eV.[34]

Most of the earlier studies concentrated on the main group of elements for the polynuclear superhalogens. Recently, superhalogens with multiple transition metal atoms at the core are drawing more and more attention. For example, $Ta_3F_{16}^-$ was found to have a VDE value of 12.63 eV.[20] This cluster can be viewed as $(TaF_5)_3F^-$ where the maximal valence of Ta is +5. Similar properties have recently been observed in Mn_xCl_y clusters. We note that among all the transition metal elements, Mn plays a unique role in superhalogen studies due to its varying oxidation numbers from 0 to +7 or even negative.[35] In particular, Mn exhibits a $3d^54s^2$ electronic configuration and in the +2 valence state forms the basis of molecular magnets with magnetic moments of 5 μ_B per atom. A search for magnetic superhalogens led to a study of the mass spectra of Mn_xCl_y clusters which revealed high peaks for $(MnCl_2)_xCl^-$ (x = 1–4) composition.[36] Theoretical calculations performed for x = 1–3 composition[36] showed that these peaks arise due to the anomalously high electron affinities and hence for the enhanced stability of these anions.

Recently, another new class of species was found to have electron affinities even larger than those of superhalogens. These moieties called "hyperhalogens"[37–42] consist of a central metal atom surrounded by superhalogen moieties. We wondered if for some specific composition polynuclear species may be the same as hyperhalogens. To illustrate this concept we concentrate on Mn_xCl_y systems. Since $MnCl_3$ cluster is a superhalogen one can expect that $Mn(MnCl_3)_x$ ($x \geq 3$) clusters will behave as hyperhalogens. To find out for what value of x in $Mn(MnCl_3)_x$ clusters can also be viewed as a polynuclear species with composition $(MnCl_2)_yCl$, we equate:

$$Mn(MnCl_3)_x = (MnCl_2)_yCl.$$

a)Author to whom correspondence should be addressed. Electronic mail: qianwang2@pku.edu.cn.

This leads to a unique value of x, namely, $x = 3$, i.e., Mn_4Cl_9 can be viewed either as $[Mn(MnCl_3)_3]$ or $(MnCl_2)_4Cl$. In previous work neither theoretical calculations nor experimental measurements of photo-electron spectra were performed for Mn_4Cl_9. Since the additional electron in $Mn_4Cl_9^-$ could not be photodetached with the 6.4 eV laser, it suggests that the electron affinity of Mn_4Cl_9 must be higher than 6.4 eV. To see if this is indeed the case we studied the geometries and electronic structure of neutral and negatively charged Mn_4Cl_9. We not only found its electron affinity to be higher than that of Cl, but that it is also higher than that of $MnCl_3$. In addition, the geometry of $Mn(MnCl_3)_3^-$ resembles more of a Mn atom at the center surrounded by three $MnCl_3$ moieties instead of a $[MnCl_2]_4$ moiety to which a Cl atom is attached. Thus, Mn_4Cl_9 can be classified as a hyperhalogen. It is important to note that previously discussed hyperhalogens have all consisted of three elements. Here Mn_4Cl_9 represents the first binary species having hyperhalogen behavior. In addition, Mn being a transition metal atom that carries a large magnetic moment, these hyperhalogens provide the possibility of designing molecular magnets with large electron affinities.

COMPUTATIONAL METHODS

Our calculations were carried out using GAUSSIAN 09 code.[43] Geometry optimization and frequency analysis were performed at B3LYP/6-311+G* level.[44–46] To search for the ground state of Mn_4Cl_9 and its anion species, we selected about 20 initial geometrical configurations and optimized each structure without any symmetry constraint. The low-lying isomers ($\Delta E < 5$ kcal/mol) of $Mn_4Cl_9^-$ were then further re-optimized for each possible spin state using the PBE0 hybrid exchange-correlation functional[47] with aug-cc-pVTZ basis set[48] for Cl and SDD basis set and pseudopotential[49,50] for Mn. For comparison with earlier results, calculations were also performed for $Mn_kCl_{2k+1}^-(k = 1 \sim 4)$. To validate the consistency of our results with PBE0, VDEs were calculated at the B3LYP/6-311+G*, B3LYP/6-311+G(3df), and OVGF/6-311+G*//PBE0/Mn/SDD/Cl/aug-cc-pVTZ level.[51–53] For $Mn_kCl_{2k+1}^-(k = 1, 2)$, UHF-CCSD(T)/Mn/SDD/Cl/aug-cc-pVTZ// PBE0/Mn/SDD/Cl/aug-cc-pVTZ level of theory has also been used.[54] Zero point energy (ZPE) corrections were calculated by using B3LYP/6-311+G*. We compared the experimental and theoretical VDEs for $Mn_kCl_{2k+1}^-(k = 1, 2)$ to confirm the reliability of our theoretical methods. The natural bond orbital (NBO) analysis[55,56] was performed for bonding and charge discussions, and GaussView 5.0.8 and VMD 1.9.1[57] were used for structure and molecular orbital (MO) visualization.

RESULTS AND DISCUSSION

We begin our discussions with the optimized structures of both the neutral and anionic Mn_4Cl_9 as shown in Figures 1 and 2. Extensive search revealed the trophy-shaped structure (Fig. 1(a)) to be the lowest energy isomer of anionic $Mn_4Cl_9^-$. On the other hand, the ground-state geometry of neutral Mn_4Cl_9 completely differs from that of its anion displaying an open, linear structure (Fig. 2(a)). The ground-state geometries for both neutral and anionic Mn_4Cl_9 have three Mn atoms with fourfold coordination while the fourth Mn atom is threefold coordinated.

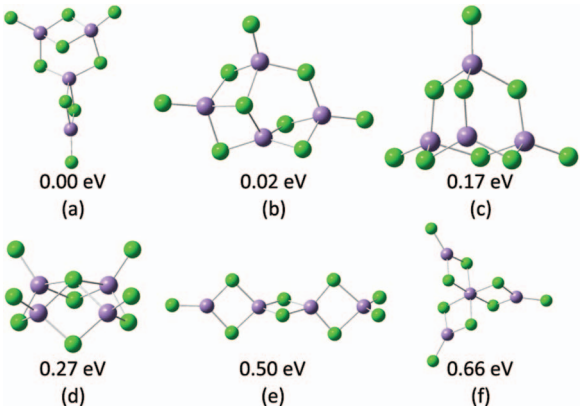

FIG. 1. Optimized geometry of isomers of the anionic $Mn_4Cl_9^-$ and their ZPE corrected relative energies at B3LYP/6-311+G* level.

To refine the geometries of the isomers, optimizations at PBE0/Mn/SDD/Cl/aug-cc-pVTZ were carried out. Three energetically degenerate structures were found as shown in Figure 3, where the trophy-shaped structure (Fig. 3(a)) is again the lowest-energy configuration; the second isomer has nearly the same energy ($\Delta E = 0.01$ eV) and the third one is only 0.06 eV higher in energy as compared to the first one. The magnetic couplings between Mn atoms in all the three structures are antiferromagnetic, resulting in the total magnetic moments of 0 μ_B. The ground-state structure of anionic Mn_4Cl_9 has C_1 symmetry, where Mn-Mn distance is different for the different spin orientations. The low-lying isomer (Figure 3(c)) has C_{2v} symmetry having a diamond-like shape. Based on our calculations, we found that the smaller 6-311G basis sets would underestimate the spin magnetic moments. Therefore, we used PBE0/Mn/SDD/Cl/aug-cc-pVTZ for magnetic moment and orbital analyses.

The Mulliken atomic spin density distribution for the ground-state structures of anionic Mn_4Cl_9 as well as neutral Mn_4Cl_9 are given in Figure 4, indicating that the majority of the spin moments reside on the four Mn

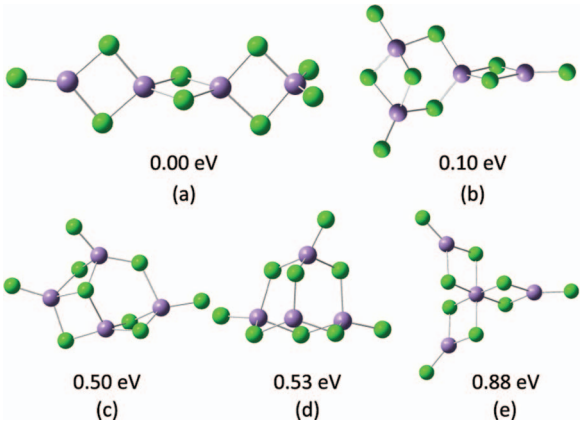

FIG. 2. Optimized structures of isomers of the neutral Mn_4Cl_9 and their ZPE corrected relative energies at B3LYP/6-311+G* level.

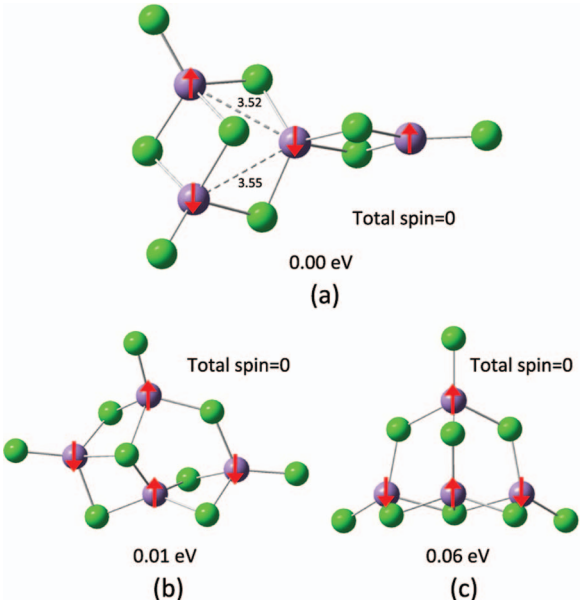

FIG. 3. Re-optimized structures of three energetically nearly degenerate isomers of the anionic Mn_4Cl_9 and their ZPE corrected relative energies at PBE0/Mn/SDD/Cl/aug-cc-pVTZ. The arrows indicate the direction of local spin moments.

atoms. As stated above, the spin coupling in anionic Mn_4Cl_9 is antiferromagnetic, where the four Mn atoms carry magnetic moments of 5.00 μ_B, −5.12 μ_B, 5.03 μ_B, and −5.02 μ_B, respectively. We note that in $Mn_4Cl_9^-$, the corresponding α spin electron configurations of the four Mn atoms are $[Ar]4s^{0.19}3d^{4.94}4p^{0.21}$, $[Ar]4s^{0.14}3d^{0.43}4p^{0.28}$, $[Ar]4s^{0.18}3d^{4.91}4p^{0.27}$, and $[Ar]4s^{0.13}3d^{0.35}4p^{0.23}$, while the β spin electron configurations of the four Mn atoms are $[Ar]4s^{0.13}3d^{0.29}4p^{0.19}$, $[Ar]4s^{0.17}3d^{4.85}4p^{0.30}$, $[Ar]4s^{0.15}3d^{0.35}4p^{0.25}$, and $[Ar]4s^{0.19}3d^{4.91}4p^{0.28}$, respectively. It is therefore clear that although the main contributions to the moments come from 3*d* orbitals, due to the *s-p-d* hybridization, the 4*s* and 4*p* orbitals are slightly polarized,

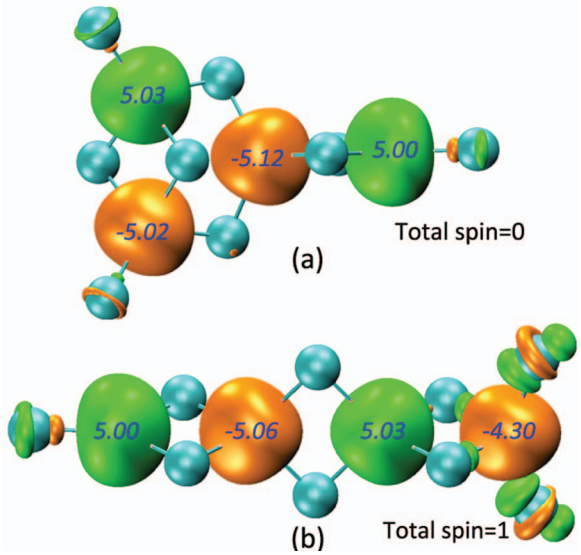

FIG. 4. Spin density distribution in (a) $Mn_4Cl_9^-$, (b) Mn_4Cl_9 (isosurface value is 0.005). Magnetic moments (μ_B) at the Mn sites are shown in italics.

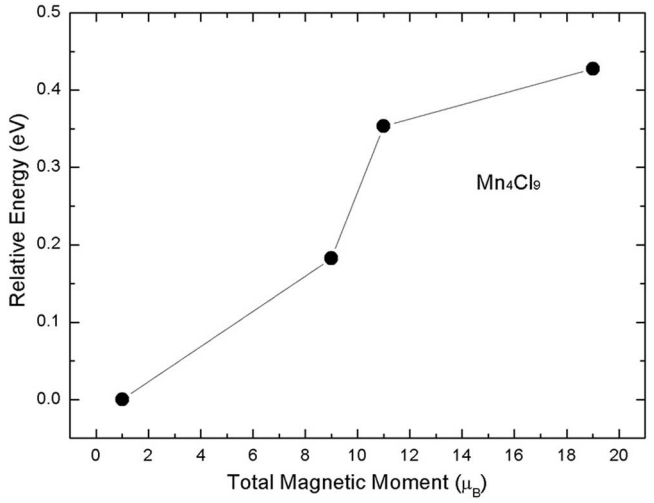

FIG. 5. Energies of neutral Mn_4Cl_9 states with different total spin given with respect to the global-minimum state.

resulting in large total magnetic moments on Mn sites. However, when one electron is removed from the anion, the *s-p-d* hybridization is reduced. Consequently, the spin couplings between Mn sites become ferrimagnetic with the total magnetic moment of 1 μ_B and the corresponding moments at the four Mn sites are 5.00 μ_B, −5.06 μ_B, 5.03 μ_B, and −4.30 μ_B respectively. The relative energies of Mn_4Cl_9 for different possible spin states calculated with respect to the lowest-energy spin configuration are shown in Figure 5. The doublet spin state with three AFM coupled Mn pairs is found to be the energy minimum, which is analogous to the results obtained from the previous analysis of Mn_2Cl_5 and Mn_3Cl_7.[36]

From the above calculations we can see that the anionic Mn_4Cl_9 is an antiferromagnetic molecular magnet. To have further insight into its stability and the oxidation property of its neutral counterpart, we used B3LYP and PBE0 hybrid functional with various basis sets to calculate the VDEs of anionic $Mn_xCl_{2x+1}(x = 1\sim4)$ clusters. Outer valence Green's function (OVGF) and coupled cluster with single and double and perturbative triple excitations (CCSD(T)) methods were also employed for comparisons. Theoretical VDEs obtained at different levels of theory are compared with experimental values of $Mn_xCl_{2x+1}(x = 1\sim2)$ in Table I. Just as expected, the VDEs of anionic $Mn_xCl_{2x+1}(x = 1\sim4)$ increase with the value *x*. For $x = 1$, the calculated VDE is 5.27 eV at the PBE0/Mn/SDD/Cl/aug-cc-pvtz level, whereas the calculated VDE for $x = 4$ is found to increase to 6.76 eV. Unfortunately, this cannot be compared with the previous experiment due to the limitation of the PES photon energy used.[29,36] Our theoretical results for $x = 1$ and $x = 2$, however, are in good agreement with previous calculations as well as experimental PES results,[36] suggesting that it is reasonable to employ DFT method within hybrid density functional to acquire theoretical VDE for anionic Mn_4Cl_9. As can be seen, the VDEs for all the anionic $Mn_xCl_{2x+1}(x = 1\sim4)$ species greatly exceed the EA of chlorine atom and thus may be classified as superhalogens. However, they do not belong to conventional superhalogens and can be considered as $(MnCl_2)_xCl$ as is pointed out in previous effort.[36]

TABLE I. Comparison between experimental and calculated VDEs values of $Mn_kCl^-_{2k+1}(k = 1\sim4)$. All energies are in eV.

	B3LYP/ 6-311G*	B3LYP/ 6-311+G(3df)	PBE0/ 6-311G*	PBE0/Mn/SDD/ Cl/aug-cc-pVTZ	OVGF[a]	UHF- CCSD(T)[b]	ROHF- CCSD(T)[c]	EOMCCSD[d]
$MnCl_3^-$	5.18	5.05	5.31	5.27(5.6±0.1)[e]	5.65	5.83	5.68	5.79
$Mn_2Cl_5^-$	6.10	5.98	6.24	6.21(6.3±0.1)[e]	6.69	6.76	[f]	[f]
$Mn_3Cl_7^-$	6.37	6.25	6.54	6.51	7.18	[f]	[f]	[f]
$Mn_4Cl_9^-$	6.61	6.54	6.77	6.76	7.24	[f]	[f]	[f]

[a]VDEs were calculated at OVGF/6-311+G*//PBE0/Mn/SDD/Cl/aug-cc-pvtz level.
[b]VDEs were calculated at UHF-CCSD(T)/Mn/SDD/Cl/aug-cc-pvtz//PBE0/Mn/SDD/Cl/aug-cc-pvtz level.
[c]VDEs were calculated at ROHF-CCSD(T)/Mn/SDD/Cl/aug-cc-pvtz//PBE0/Mn/SDD/Cl/aug-cc-pvtz level.
[d]VDEs were calculated at EOMCCSD/Mn/SDD/Cl/aug-cc-pvtz//PBE0/Mn/SDD/Cl/aug-cc-pvtz level.
[e]VDEs in parentheses are experimental values.[36]
[f]VDE could not be calculated at this level of theory.

That the VDEs of polynuclear superhalogens become larger with the increasing core size has inspired growing interest in the search of superhalogens with extremely high VDEs for oxidation of materials with large ionization potential. Hyperhalogens also provide a means of creating species with ever increasing electron affinities, but a link between these two concepts has not yet been demonstrated. Here we present a structural-based hypothesis to elucidate the unconventionally high VDE for anionic Mn_4Cl_9. $MnCl_3$ is a typical high spin superhalogen since the preferred oxidation state of Mn in Mn halides is +2.[35] If we take $MnCl_3$ as a structural block, Mn_2Cl_5 can be understood as $Mn(MnCl_3)Cl_2$, Mn_3Cl_7 as $Mn(MnCl_3)_2Cl$, and Mn_4Cl_9 as $Mn(MnCl_3)_3$. In each of these clusters the core is a Mn atom and halogen (Cl) atoms are successively replaced by $MnCl_3$ superhalogen moieties. Thus, it is expected that the VDE of $Mn_kCl^-_{2k+1}(k = 1\sim4)$ increases as the number of Mn atoms getting larger. All these results except for Mn_4Cl_9 have been previously confirmed. If the above analysis will hold for Mn_4Cl_9 it can be classified as a hyperhalogen composed of only two elements. We define such kind of hyperhalogens as binary hyperhalogen because there is only one element acting as both the central atom of the hyperhalogen and the central atom of the superhalogen moieties.

It is therefore appropriate to presume that the ground-state geometry for anionic Mn_4Cl_9 involves a central Mn atom chelated by three $MnCl_3$ blocks with every $MnCl_3$ fragment providing two Cl bridging atoms, forming a highly symmetric octahedral structure. However, based on B3LYP calculation, the octahedral form (Fig. 1(f)) was found to be higher in energy than the trophy-shaped framework (Fig. 1(a)) by 0.66 eV. We attribute this to an intrinsic property of central metal cation, namely, coordination number. Mn^{2+} is most likely to display the coordination number of 4 in its halides,[35] thus preferring the sp^3 hybridization as well as tetragonal geometry. Our calculations show that the global minimum structure for the anionic Mn_4Cl_9 is determined by its hyperhalogen

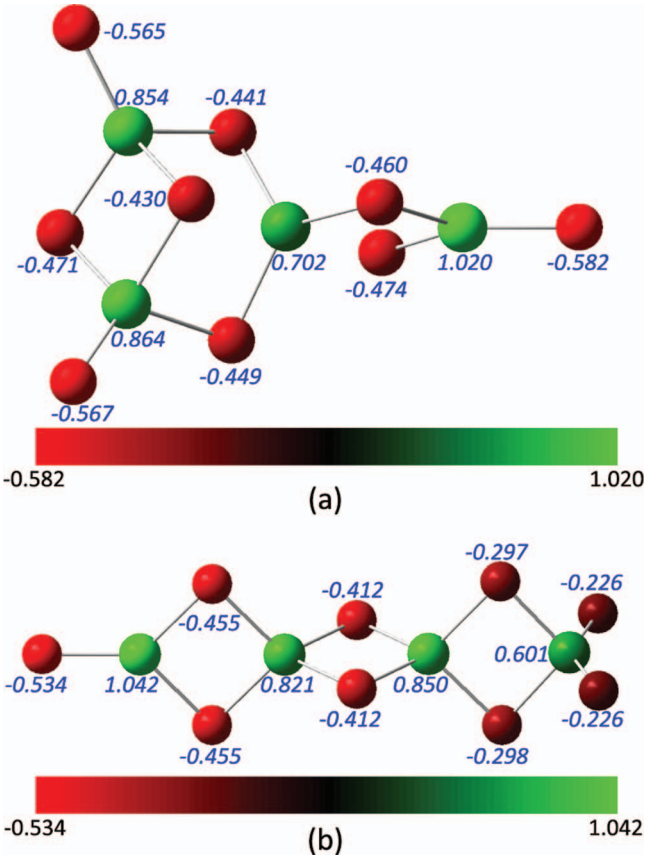

FIG. 6. NBO charge distribution of the $Mn_4Cl_9^-$ (a) and Mn_4Cl_9 (b).

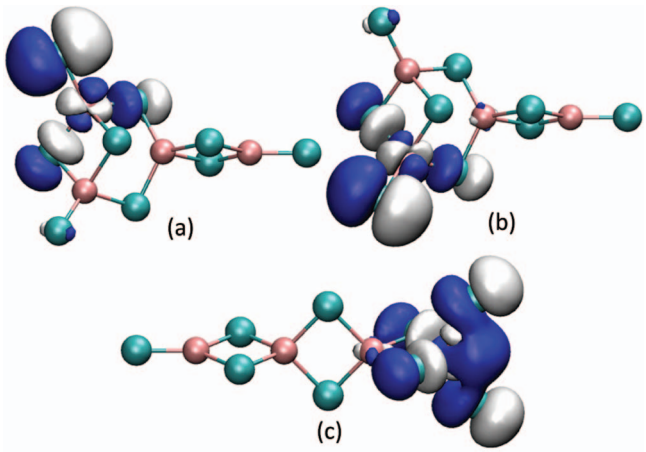

FIG. 7. Highest occupied α orbital (a), highest occupied β orbital (b) of the anionic Mn_4Cl_9, and lowest unoccupied β orbital (c) of the neutral Mn_4Cl_9.

TABLE II. Comparison of VDEs for X^- and LiX_2^- (X = F, BO_2, Mn_4Cl_9).

Anions	F^-	BO_2^-	$Mn_4Cl_9^-$	LiF_2^-	$LiFBO_2^-$	$Li(BO_2)_2^-$	$Li(Mn_4Cl_9)_2^-$
VDE (eV)	3.65	4.14	6.76	5.44	5.66	5.80	7.26

nature as well as the coordination number of Mn^{2+}. Thus, the Mn_4Cl_9 is different from the conventional hyperhalogens.

In order to have a better understanding of the nature of bonding and electronic structure in the neutral and negatively charged Mn_4Cl_9, we calculated the electron distribution by analyzing the NBO charge. The results for neutral and anionic Mn_4Cl_9 are presented in Figure 6. We can clearly see that the charges on all the Mn atoms are positive while they are negative on all the Cl atoms, resulting from the anticipated Mn to Cl charge transfer. However, owing to partial back electron transfer from Mn to Cl, the Mn–Cl bonds have a somewhat covalent nature. This is confirmed by the relatively smaller charges on Mn and Cl atoms compared to other metal halides. The Cl atoms are, therefore, slightly polarized and also carry small spin magnetic moments (Figure 4). Particularly, the central Mn atom in the anionic Mn_4Cl_9 and the fourfold coordinated terminal Mn atom in the neutral Mn_4Cl_9 involve more of their 3*d* electrons in the Mn–Cl interactions, as it can be seen from the smaller NBO charges compared to other Mn atoms. The total charges on all the Mn atoms in the negatively charged Mn_4Cl_9 and its neutral counterpart are +3.44 e and +3.31 e, respectively. This clearly indicates that the extra electron in the anionic Mn_4Cl_9 is delocalized over the Cl atoms, which contributes considerably to the high VDE of anionic Mn_4Cl_9. MO analysis indicates that the highest occupied α and β spin orbitals of anionic Mn_4Cl_9 are energetically nearly degenerate and mainly consist of the terminal Cl p_x orbital and the adjacent Mn $d_{x^2-y^2}$ orbital, while the lowest unoccupied β spin orbital is mostly contributed by the fourfold coordinated terminal Mn d_{xz} orbital and the peripheral Cl p_x orbitals, as illustrated in Figure 7.

To further explore the possibility that the Mn_4Cl_9 can serve as a building block for larger clusters, we calculated the equilibrium structure and VDE of anionic $Li(Mn_4Cl_9)_2$ cluster. The ground state geometry of anionic $Li(Mn_4Cl_9)_2$ cluster (Fig. 8) is linear, where bond lengths of the two Mn_4Cl_9 fragments are nearly identical with those of the free anionic Mn_4Cl_9, indicating that the Mn_4Cl_9 anion is highly stable. We then compared the VDE of anionic $Li(Mn_4Cl_9)_2$ with several other superhalogen and hyperhalogen anions to find out whether the anionic $Li(Mn_4Cl_9)_2$ exhibited an ultrahyperhalogen nature. The results are given in Table II. At the same level of theory, $Li(Mn_4Cl_9)_2$ anion possesses a high VDE of 7.26 eV which is much larger than that of LiF_2 or $Li(BO_2)_2$ anion. Furthermore, the VDE of $Li(Mn_4Cl_9)_2$ anion even exceeds that of the free Mn_4Cl_9 anion, which supports the conclusion that the $Li(Mn_4Cl_9)_2$ is indeed an ultrahyperhalogen. From the calculated VDEs in Table II, it is also obvious that the VDEs of the LiX_2^- clusters increase as the ligands having higher VDEs. It is thus worth employing superhalogens or hyperhalogens as building blocks of clusters with unprecedented oxidizing property. The fragmentation energy of $Li(Mn_4Cl_9)_2$ corresponding to the lowest energy pathway is 11.56 eV. Consequently, anionic $Li(Mn_4Cl_9)_2$ is thermodynamically stable. Thus, it should be possible to synthesize these in experiments.

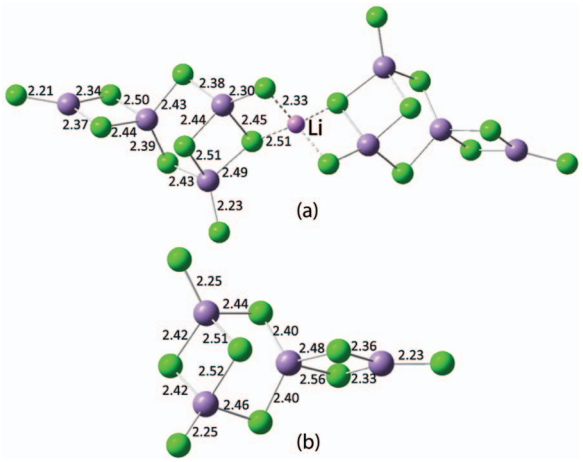

FIG. 8. Optimized geometries of $Li(Mn_4Cl_9)_2^-$ (a) and $Mn_4Cl_9^-$ (b). All bond lengths are in (Å).

CONCLUSIONS

In summary, we have systematically studied the equilibrium geometries, magnetic couplings, vertical detachment energies, and the charge distributions of Mn_4Cl_9 and its anion by using density functional theory based calculations. The following conclusions are drawn: (1) There exists a unique composition of Mn_xCl_y where the cluster can be simultaneously termed as a binary hyperhalogen or a polynuclear superhalogen. In this case Mn_4Cl_9 is such a cluster. (2) The ground state geometry of Mn_4Cl_9 anion can be viewed as $Mn(MnCl_3)_3$ with some distortions. Since the $MnCl_3$ behaves like a magnetic superhalogen with Mn atom carrying a magnetic moment of 5 μ_B, Mn_4Cl_9 anion can be called a magnetic hyperhalogen. This is a unique binary system since previously studied hyperhalogens consisted of three or more elements like $Au(BO_2)_2$ and were not magnetic. (3) In the anionic Mn_4Cl_9, the magnetic couplings between Mn atoms are antiferromagnetic and each Mn site carries a moment of about 5 μ_B. Cl sites are slightly spin polarized, sharing similar features with Mn_2Cl_5 and Mn_3Cl_7. (4) Natural bonding orbital analysis demonstrates the partial covalent nature of Mn–Cl interactions. (5) The Mn_4Cl_9 can be used as a ligand to design ultra-hyperhalogen moieties. By varying the ligand X from F to BO_2 to Mn_4Cl_9, the VDE of LiX_2^- can be seen to steadily increase from 5.44 eV to 5.80 eV to 7.26 eV. We hope that our study will stimulate more experimental efforts to better understand binary hyperhalogens with varying size.

ACKNOWLEDGMENTS

This work is supported by grants from the National Natural Science Foundation of China (Grant Nos. NSFC-21273012 and NSFC-11174014), the National Grand Fundamental Research 973 Program of China (Grant No. 2012CB921404), and from the (U.S.) Department of Energy.

[1]F. Wudl, Acc. Chem. Res. **17**, 227 (1984).
[2]A. I. Marshakov, N. P. Chebotareva, and N. B. Lukina, Prot. Met. **28**, 301 (1992).
[3]N. Bartlett, G. Lucier, C. Shen, W. J. Casteel, Jr., L. Chacon, J. Munzenberg, and B. Žemva, J. Fluorine Chem. **71**, 163 (1995).
[4]N. Bartlett, Proc. Chem. Soc., London 218 (1962).
[5]M. V. Korobov, S. V. Kuznetsov, L. N. Sidorov, V. A. Shipachev, and V. N. Mit'kin, Int. J. Mass. Spectrom. Ion Process. **87**, 13 (1989).
[6]H. Hotop and W. C. Lineberger, J. Phys. Chem. Ref. Data **14**, 731 (1985).
[7]G. L. Gutsev and A. I. Boldyrev, Chem. Phys. **56**, 277 (1981).
[8]G. Gutsev and A. I. Boldyrev, Russ. Chem. Rev. **56**, 519 (1987).
[9]G. L. Gutsev and A. I. Boldyrev, Chem. Phys. Lett. **84**, 352 (1981).
[10]G. L. Gutsev and A. I. Boldyrev, Chem. Phys. Lett. **108**, 250 (1984).
[11]G. L. Gutsev and A. I. Boldyrev, J. Phys. Chem. **94**, 2256 (1990).
[12]V. G. Zakrzewski and A. I. Boldyrev, J. Chem. Phys. **93**, 657 (1990).
[13]G. L. Gutsev, Chem. Phys. Lett. **184**, 93 (1991).
[14]J. V. Ortiz, J. Chem. Phys. **99**, 6727 (1993).
[15]G. L. Gutsev, R. J. Bartlett, A. I. Boldyrev, and J. Simons, J. Chem. Phys. **107**, 3867 (1997).
[16]G. L. Gutsev, P. Jena, and R. J. Bartlett, Chem. Phys. Lett. **292**, 289 (1998).
[17]I. Anusiewicz and P. Skurski, Chem. Phys. Lett. **358**, 426 (2002).
[18]S. T. Arnold, T. M. Miller, and A. A. Viggiano, Int. J. Mass Spectrom. **218**, 207 (2002).
[19]I. Anusiewicz, M. Sobczyk, I. Dabkowska, and P. Skurski, Chem. Phys. **291**, 171 (2003).
[20]M. Sobczyk, A. Sawicka, and P. Skurski, Eur. J. Inorg. Chem. **2003**, 3790 (2003).
[21]C. Sikorska, S. Smuczynska, P. Skurski, and I. Anusiewicz, Inorg. Chem. **47**, 7348 (2008).
[22]S. Smuczynska and P. Skurski, Chem. Phys. Lett. **452**, 44 (2008).
[23]X.-B. Wang, C.-F. Ding, L.-S. Wang, A. I. Boldyrev, and J. Simons, J. Chem. Phys. **110**, 4763 (1999).
[24]X.-B. Wang and L.-S. Wang, J. Phys. Chem. A **104**, 4429 (2000).
[25]X.-B. Wang and L.-S. Wang, J. Chem. Phys. **113**, 10928 (2000).
[26]G. L. Gutsev, P. Jena, H.-J. Zhai, and L.-S. Wang, J. Chem. Phys. **115**, 7935 (2001).
[27]D. E. Bergeron, A. W. Castleman, T. Morisato, and S. N. Khanna, Science **304**, 84 (2004).
[28]B. M. Elliott, E. Koyle, A. I. Boldyrev, X.-B. Wang, and L.-S. Wang, J. Phys. Chem. A **109**, 11560 (2005).
[29]J. Yang, X.-B. Wang, X.-P. Xing, and L.-S. Wang, J. Chem. Phys. **128**, 201102 (2008).
[30]Y.-L. Wang, X.-B. Wang, X.-P. Xing, F. Wei, J. Li, and L.-S. Wang, J. Phys. Chem. A **114**, 11244 (2010).
[31]A. N. Alexandrova, A. I. Boldyrev, Y.-J. Fu, X. Yang, X.-B. Wang, and L.-S. Wang, J. Chem. Phys. **121**, 5709 (2004).
[32]I. Anusiewicz and P. Skurski, Chem. Phys. Lett. **440**, 41 (2007).
[33]I. Anusiewicz, Aust. J. Chem. **61**, 712 (2008).
[34]S. Freza and P. Skurski, Chem. Phys. Lett. **487**, 19 (2010).
[35]K. Pradhan, G. L. Gutsev, C. A. Weatherford, and P. Jena, J. Chem. Phys. **134**, 234311 (2011).
[36]M. M. Wu, H. Wang, Y. J. Ko, Q. Wang, Q. Sun, B. Kiran, A. K. Kandalam, K. H. Bowen, and P. Jena, Angew. Chem., Int. Ed. **50**, 2568 (2011).
[37]M. Willis, M. Goetz, A. K. Kandalam, G. F. Gantefoer, and P. Jena, Angew. Chem., Int. Ed. **49**, 8966 (2010).
[38]M. Goetz, M. Willis, A. K. Kandalam, G. F. Gantefoer, and P. Jena, ChemPhysChem **11**, 853 (2010).
[39]Y. Feng, H.-G. Xu, W. Zheng, H. Zhao, A. K. Kandalam, and P. Jena, J. Chem. Phys. **134**, 094309 (2011).
[40]C. Paduani, M. M. Wu, M. Willis, and P. Jena, J. Phys. Chem. A **115**, 10237 (2011).
[41]B. Pathak, D. Samanta, R. Ahuja, and P. Jena, ChemPhysChem **12**, 2423 (2011).
[42]K. Pradhan and P. Jena, J. Chem. Phys. **135**, 144305 (2011).
[43]M. J. Frisch, G. W. Trucks, and H. B. Schlegel *et al.*, GAUSSIAN 09, Revision C.01, Gaussian, Inc., Wallingford, CT, 2010.
[44]A. D. Becke, J. Chem. Phys. **98**, 5648 (1993).
[45]R. Krishnan, J. S. Binkley, R. Seeger, and J. A. Pople, J. Chem. Phys. **72**, 650 (1980).
[46]A. D. McLean and G. S. Chandler, J. Chem. Phys. **72**, 5639 (1980).
[47]C. Adamo and V. Barone, J. Chem. Phys. **110**, 6158 (1999).
[48]R. A. Kendall, J. Thom H. Dunning, and R. J. Harrison, J. Chem. Phys. **96**, 6796 (1992).
[49]P. Schwerdtfeger, M. Dolg, W. H. E. Schwarz, G. A. Bowmaker, and P. D. W. Boyd, J. Chem. Phys. **91**, 1762 (1989).
[50]M. Dolg, U. Wedig, H. Stoll, and H. Preuss, J. Chem. Phys. **86**, 866 (1987).
[51]V. G. Zakrzewski and J. V. Ortiz, Int. J. Quantum Chem. **53**, 583 (1995).
[52]J. V. Ortiz, J. Chem. Phys. **89**, 6348 (1988).
[53]V. G. Zakrzewski, O. Dolgounitcheva, and J. V. Ortiz, J. Chem. Phys. **105**, 5872 (1996).
[54]G. D. Purvis and R. J. Bartlett, J. Chem. Phys. **76**, 1910 (1982).
[55]A. E. Reed, L. A. Curtiss, and F. Weinhold, Chem. Rev. **88**, 899 (1988).
[56]E. D. Glendening, A. E. Reed, J. E. Carpenter, and F. Weinhold, NBO Version 3.1.
[57]W. Humphrey, A. Dalke, and K. Schulten, J. Mol. Graphics **14**, 33 (1996).